

On Distinguishing Radions from Higgs Bosons

Prasanta Kumar Das^a, Santosh Kumar Rai^b and Sreerup Raychaudhuri^b

^a Department of Physics, Chung Yuan Christian University,
22 Pu-Jen, Pu-chung Li, Chung-Li (32023), Taiwan, R.O.C.

Electronic address: pdas@phys.cycu.edu.tw

^b Department of Physics, Indian Institute of Technology, Kanpur 208016, India.

Electronic addresses: sreerup@iitk.ac.in, skrai@iitk.ac.in

ABSTRACT

Radion couplings are almost identical to Higgs boson couplings, making it very difficult to distinguish the two states when the radion mass and vacuum expectation value are similar to those of the Higgs boson. The only real difference lies in the fact that the coupling of radions to off-shell fermions is proportional to the momentum rather than the mass of the fermion. This extra contribution gets cancelled in all tree-level processes and shows up only in loop-induced processes like $\Phi \rightarrow \gamma\gamma$ and $\Phi \rightarrow gg$. We perform a careful calculation of the branching ratios and establish that they can prove crucial in clearly distinguishing a radion from a Higgs boson. This claim is made concrete by evaluating the exclusive cross-sections in a radiative process involving elementary scalars.

In recent years the two-brane model of Randall and Sundrum[1] has attracted a great deal of attention because it provides an elegant solution to the thirty-odd year-old hierarchy problem of high energy physics. The most attractive feature of the 1+4 dimensional Randall-Sundrum (RS) model is that it explains the large hierarchy between the electroweak scale (0.1 – 1 TeV) and the Planck scale (10^{16} TeV) in terms of an exponential damping of the gravitational field across a small compact fifth dimension, without recourse to unnaturally large numbers¹. Since the hierarchy of scales is generated by an exponential damping across the fifth dimension, the size of this dimension requires to be just at the right value to ensure that the hierarchy is indeed a factor of $\frac{M_{Pl}}{M_{ew}} \sim 10^{16}$. Since the fifth dimension has the topology of a once-folded circle, with two D_3 -branes at the fixed points, this amounts to fixing the

¹However, it is only fair to mention that this is achieved at the expense of a delicate fine-tuning of the five-dimensional cosmological constant with the energy densities on two branes at opposite ends of the fifth dimension.

distance R_c between the two branes very precisely. This, in turn, would require a mechanism to protect the radius against large quantum corrections. The absence of such a mechanism is a major flaw in the original braneworld model of Arkani-Hamed, Dimopoulos and Dvali[2]. The question was left unresolved even in the original work[1] of RS, but an elegant model to explain this was given shortly afterwards by Goldberger and Wise[3]. They used the simple device of generating a force between the two branes which would ensure equilibrium when the distance between them is precisely the radius R_c required to generate the required hierarchy. Because of the folded structure of the fifth dimension, it is only necessary to generate an attractive force between the branes — since each brane is, topologically speaking, on *both* sides of the other, the two pulls will balance at the equilibrium point. The attractive force is modelled by postulating the time-honoured device of a scalar field which lives in all five dimensions (bulk) and has quartic self-interactions, in the bulk, as well as in projection on the branes. It is necessary only to tune the vacuum expectation values (vev's) of the scalar field on the two branes to get an attractive force as required. In fact, it can be easily shown that the potential has an extremely steep minimum at the argument R_c , indicating that the hierarchy is fixed very accurately for small oscillations of the bulk size about this minimum.

An important consequence of the (original) RS model is that there exists on the TeV-brane (which represents the observable Universe), a scalar field Φ , which is very much like a dilaton field and has been dubbed the *radion*. The RS metric, with radial fluctuations, is written in the form

$$ds^2 = e^{-2KT(x)\varphi} g_{\mu\nu}(x)dx^\mu dx^\nu - [T(x)]^2 d\varphi^2 \quad (1)$$

where $T(x)$ is a modulus field representing dilatation of the bulk, K is the bulk curvature and φ is an angular coordinate describing the fifth dimension. We can now show[4] that the five-dimensional Einstein-Hilbert action reduces, in four dimensions, to a theory with Kaluza-Klein gravity and a scalar term

$$S_\Phi = \int d^4x \sqrt{-|g|} \frac{1}{2} \partial_\mu \Phi(x) \partial^\mu \Phi(x) \quad (2)$$

where the (massless, free) scalar field

$$\Phi(x) = \sqrt{24M_5^3/K} e^{-\pi KT(x)} \quad (3)$$

is the radion field. The Goldberger-Wise stabilisation mechanism, with a bulk scalar field $B(x, \varphi)$ then creates an effective scalar Φ^4 -potential for the radion field $\Phi(x)$ with a minimum at $\langle T(x) \rangle = R_c$, where $K R_c \simeq 11.7$, the value required to generate the electroweak hierarchy.

This potential includes a radion mass term $m_\Phi^2 \Phi^2$ where m_Φ is determined by the mass m_B and couplings of the bulk scalar field. Though m_B is unknown, arguing[3] that m_B should be of the order of the Planck scale — which is the only fundamental scale in the RS model — leads to the result that m_Φ should be of the order of the electroweak symmetry-breaking scale, i.e. $m_\Phi \sim 100$ GeV.

Phenomenology of the radion field[5] starts with the coupling of the radion to ordinary matter, consisting of the Standard Model (SM) fields. This interaction which arises from the usual gravitational coupling to matter, is the same as the coupling of a dilaton field, viz.,

$$\mathcal{L}(x) = -\frac{1}{\Lambda_\Phi} \Phi(x) \eta^{\mu\nu} T_{\mu\nu}(x) \quad (4)$$

where Λ_Φ is the radion vev, corresponding to the minimum of the radion potential on the TeV brane and $T_{\mu\nu}$ is the energy-momentum tensor composed of SM fields. The radion Feynman rules can, therefore, be read off from (for example), the expressions given in Ref.[6] by simply substituting the radion for the dilaton and Λ_Φ for \bar{M}_P . It turns out that the couplings are rather similar to those of Higgs fields to other SM particles, though, of course, the radion couplings originate from the couplings of the bulk scalar² while Higgs boson couplings arise from the Standard Model sector. An important — and for this work, crucial — difference arises in the fact that there are *momentum-dependent* terms in the radion coupling to matter, which are not present in the Higgs boson coupling. To see this, we write out in full the energy-momentum tensor for a scalar field $S(x)$, a fermion field $\psi(x)$ and a vector gauge field $V_\mu(x)$.

$$\begin{aligned} \eta^{\mu\nu} T_{\mu\nu} = & -2 \left[(D^\mu S)^\dagger (D_\mu S) - 2M_S^2 S^\dagger S \right] \\ & -3i\bar{\psi} \not{D}\psi + 4m_\psi \bar{\psi}\psi + \frac{3i}{2}\partial^\mu \left[\bar{\psi}\gamma_\mu\psi \right] \\ & -M_V^2 V_\mu(x)V^\mu(x) \end{aligned} \quad (5)$$

where $D^\mu = \partial^\mu + igT_a V_a^\mu$ and T_a is the gauge group generator in the appropriate representation. The explicit form of this for the Standard Model fields is given in Ref.[8]. This interaction tells us that the vertex for $\Phi(p) \rightarrow \bar{\psi}(k_1) + \psi(k_2)$ is given (in momentum space) by

$$\mathcal{L}_{\Phi\psi\bar{\psi}} = \frac{3}{2\Lambda_\Phi} \bar{u}(k_1) \left(\not{k}_1 + \not{k}_2 - \frac{8}{3}m_\psi \right) u(k_2) \Phi(p) . \quad (6)$$

²It may be noted that the vev, Λ_Φ is a free parameter arising from the couplings of the bulk scalar and has no relation to the parameter Λ_π which is strongly constrained by bounds on the graviton mass [7].

If the fermions are on-shell, we can use the Dirac equation to write the above equation as

$$\mathcal{L}_{\Phi\psi\bar{\psi}} = -\frac{m_\psi}{\Lambda_\Phi}\bar{u}(k_1)u(k_2)\Phi(p) , \quad (7)$$

which is a Yukawa coupling very reminiscent of the Higgs boson. Obviously, if the fermions are *off-shell*, the coupling is different. An immediate consequence of the above is that radions, unlike Higgs bosons can have significant couplings to light fermions, such as electrons and u, d quarks, if any of the fermions is off-shell and has large energy-momentum values.

Once produced, a massive radion will clearly decay. Being a constituent field of the metric tensor the radion couples, as described in Eqns. (4) and (5), to *all* pairs of SM particles. Naturally, only those decays which are kinematically allowed will occur. For fermionic decay modes $\Phi \rightarrow f\bar{f}$ (on-shell), the partial decay widths will be suppressed by the factor m_f^2/Λ_Φ^2 , since the fermionic states will be on-shell and the radionic coupling will be Higgs boson-like. Thus, we need to consider only the following decay channels:

$$\begin{aligned} \Phi &\longrightarrow \gamma\gamma, \, gg \\ &\longrightarrow \tau^+\tau^-, \, c\bar{c}, \, b\bar{b} \\ &\longrightarrow W^+W^-, \, Z^0Z^0, \, H^0H^0 \\ &\longrightarrow t\bar{t} \end{aligned}$$

Detailed formulae for these are given in Ref.[8]. However, in this last-mentioned work, the formulae for the decay widths $\Phi \longrightarrow \gamma\gamma, \, gg$ have been calculated assuming the coupling in Eqn.(7) rather than the one in Eqn.(6), and are, therefore, somewhat inaccurate. This is because loop-fermions will obviously be off-shell and there will be consequent modifications to the decay amplitude itself. It is worth noting that though the lighter fermions will now couple to the scalar field through their momenta rather than their masses, there is a helicity flip involved in the scalar-vector-vector one-loop diagrams, which results in an amplitude proportional to the fermion masses. As a result, it is only the top quark loop which makes any significant contribution — which is also the case with Higgs bosons. The differences arise, then, solely from the extra off-shell terms in the $\Phi t\bar{t}$ coupling.

In this work, we have calculated the one-loop-mediated decay widths afresh, using the off-shell coupling of Eqn.(6). The relevant Feynman diagrams are listed in Figure 1. Of these, the triangle diagrams marked (A) and (B) are similar to those responsible for the process $H^0 \rightarrow \gamma\gamma$. The ones marked (C) and (D) arise from non-renormalisable couplings of the radion (dilaton) to a photon and a fermion pair, which arise at the lowest order in an

effective theory of gravity coupling to matter. It is worth mentioning at this point that the presence of these vertices is responsible, in tree-level processes like, for example, $e^+e^- \rightarrow Z\Phi$ or $e^+e^- \rightarrow \ell^+\ell^-\Phi$, for precisely cancelling out the momentum-dependent part of the $\ell^+\ell^-\Phi$ coupling and rendering the cross-section totally Higgs-like. However, the situation is different inside a loop diagram, as we shall presently argue.

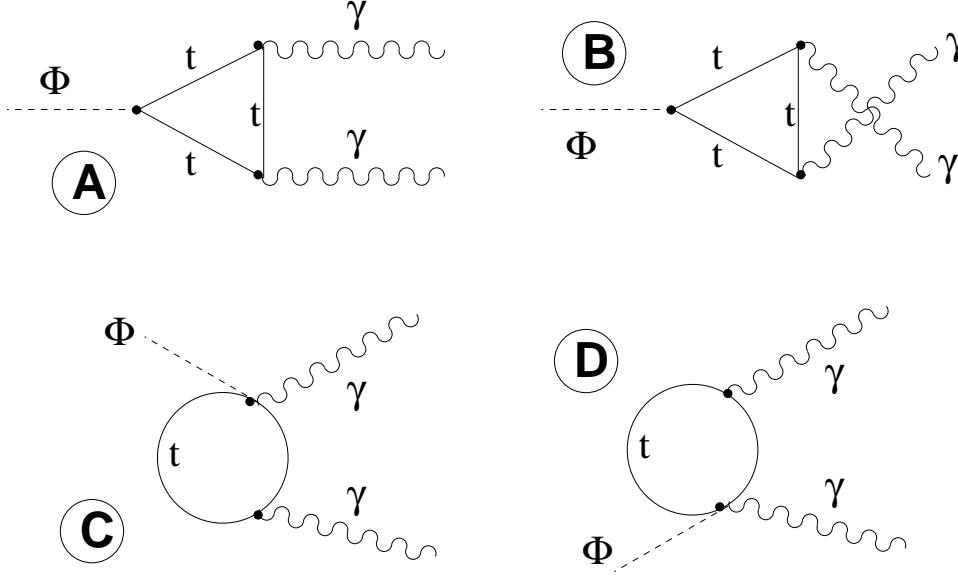


Figure 1. *Feynman diagrams with a top quark loop contributing to the process $\Phi \rightarrow \gamma\gamma$ at the one-loop level.*

Following the usual procedure[9] for calculating the amplitude for a process like $\Phi(p) \rightarrow \gamma(k_1)\gamma(k_2)$, we write the amplitude as

$$\mathcal{M}(\Phi \rightarrow \gamma\gamma) = [A(p^2)k_1^\nu k_2^\mu + B(p^2)\eta^{\mu\nu}] \varepsilon_\mu^*(k_1)\varepsilon_\nu^*(k_2) \quad (8)$$

which is consistent with Lorentz-symmetry and the transverse nature of the photon. Imposition of gauge symmetry at once leads to the Ward identity

$$B(p^2) = -A(p^2)k_1 \cdot k_2 \quad (9)$$

which relates the (naively divergent) form factor $B(p^2)$ to the finite form factor $A(p^2)$, and hence acts as a regulator for the process. The amplitude then becomes

$$\mathcal{M}(\Phi \rightarrow \gamma\gamma) = A(p^2) (k_1^\nu k_2^\mu - k_1 \cdot k_2 \eta^{\mu\nu}) \varepsilon_\mu^*(k_1)\varepsilon_\nu^*(k_2) \quad (10)$$

which means that it is only necessary to calculate the finite form factor $A(p^2) = A(M_\Phi^2)$ in order to get the decay width. Since $A(p^2)$ can be calculated by evaluating the coefficients of

$k_1^\nu k_2^\mu$ alone, it can now be seen, by writing down the Feynman amplitudes for the diagrams marked (A)–(D) in Figure 1, that the contributions to $A(p^2)$ arise from those marked (A) and (B), but not from those marked (C) and (D). Thus, the exact cancellation of momentum-dependent terms, which renders the effective radion coupling Higgs-like in the tree-level, does *not* go through at the one-loop level. This also ensures that the diagrams (A) and (B) in Figure 1 have residual momentum-dependent effects and justifies corrections to the partial decay width of Ref.[8] — which is the thrust of our present work.

For the two-photon decay mode, then, our final results are

$$\Gamma(\Phi \rightarrow \gamma\gamma) = \frac{1}{64\pi} \frac{M_\Phi^3}{\Lambda_\Phi^2} \left(\frac{\alpha}{\pi} \right)^2 |I_\gamma|^2 \quad \text{where} \quad I_\gamma = b_{QED} + I_W + \sum_f N_c Q_f^2 I_f \quad (11)$$

In the above, N_c is the number of colours of the fermion f and Q_f is the fermionic charge. The QED beta function (appearing because of the trace anomaly) is given by[10, 11]

$$\begin{aligned} b_{QED} &= \frac{20}{9} \text{ for } M_\Phi \leq 2M_W \\ &= \frac{31}{18} \text{ for } 2M_W < M_\Phi \leq 2m_t \\ &= \frac{12}{6} \text{ for } M_\Phi > 2m_t \end{aligned} \quad (12)$$

and the loop integral functions I_W and I_f are given by

$$\begin{aligned} I_W &= -1 - \frac{3}{2}\lambda_W + \frac{3}{2}\lambda_W(1 - \frac{1}{2}\lambda_W) F(\lambda_W) \\ I_f &= -8\lambda_f - \lambda_f(4\lambda_f - 1) F(\lambda_f) \end{aligned} \quad (13)$$

where $\lambda_i = (2m_i/M_\Phi)^2$, with i running over all the particles involved, and $F(\lambda)$ is given by

$$\begin{aligned} F(\lambda) &= -2 \left[\sin^{-1} \frac{1}{\sqrt{\lambda}} \right]^2 \text{ for } \lambda \geq 1 \\ &= -\frac{\pi^2}{2} + \frac{1}{2} \log^2 \frac{1 + \sqrt{1 - \lambda}}{1 - \sqrt{1 - \lambda}} - i\pi \log \frac{1 + \sqrt{1 - \lambda}}{1 - \sqrt{1 - \lambda}} \text{ for } \lambda < 1 \end{aligned}$$

This partial decay width differs from the analogous $H^0 \rightarrow \gamma\gamma$ decay width[12] in two major particulars, viz.,

- The presence of the trace anomaly, i.e. the b_{QED} term.
- A different function I_f in Eqn. (13) from that given in, for example, Ref.[12].

We now go on to calculate the very-similar process $\Phi \longrightarrow gg$, which yields a partial decay width

$$\Gamma(\Phi \rightarrow gg) = \frac{1}{64\pi} \frac{M_\Phi^3}{\Lambda_\Phi^2} \left(\frac{\alpha_s}{\pi} \right)^2 |I_g|^2 \quad \text{where} \quad I_g = b_{QCD} + \sum_f \sqrt{2} I_f \quad (14)$$

and, obviously, there is no I_W contribution. The QCD beta function is given by the usual formula

$$\begin{aligned} b_{QCD} = 11 - \frac{2}{3} N_f &= \frac{23}{3} \text{ for } M_\Phi \leq 2M_t \\ &= \frac{21}{3} \text{ for } M_\Phi > 2M_t \end{aligned} \quad (15)$$

and for α_s we take the usual running value governed by b_{QCD} .

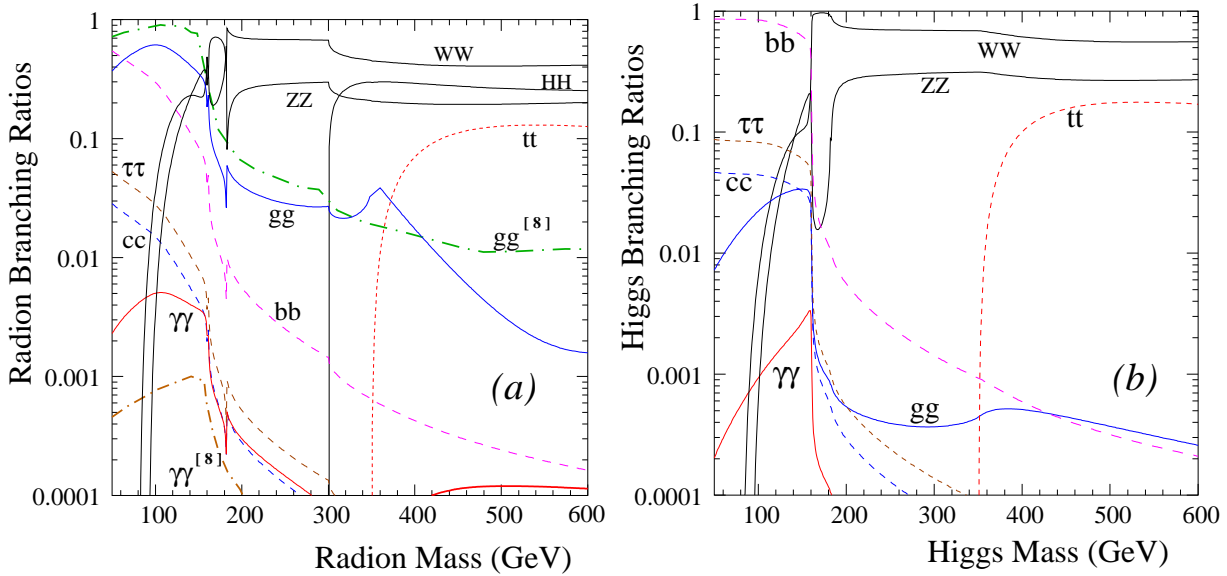


Figure 2. Branching ratios for (a) a radion and (b) a Higgs boson (of the Standard Model) as a function of the mass. Kinks at kinematic thresholds are mostly due to numerical instabilities. Note the enormous difference in the two-gluon decay mode for the two cases.

Branching ratios of the radion to different decay channels may now be calculated by combining the above formulae with those given in, for example, Ref.[8], and varying the radion mass M_Φ . Obviously there will be no dependence on the radion vev, since all the partial decay widths contain the same factor Λ_Φ^{-2} . We have exhibited our results in Figure 2(a), which show the principal branching ratios of the radion, assuming a Higgs boson mass of 150 GeV. For comparison, Figure 2(b) shows a similar set of branching ratios (except the HH decay mode) for a Standard Model Higgs boson with masses run over the same range. The dot-dashed lines marked $gg^{[8]}$ and $\gamma\gamma^{[8]}$ correspond to earlier results presented in Ref. [8]

where the momentum dependence of the radion-fermion-antifermion coupling had not been taken into account. It may be noted that the difference is quite significant, and indicates that a cancellation takes place between the finite part of the loop diagram and the trace anomaly, which is more pronounced for a heavy radion.

As the figure shows, the decay patterns of the two scalar particles in question exhibit a great deal of similarity but have some significant differences also. Once above the WW and ZZ thresholds, both decay primarily to weak bosons, with a small percentage of top-anti top decays when the corresponding threshold is crossed. Both show significant branching ratios for the WW^* and ZZ^* modes in the scalar mass range between M_W to $2M_W$ and M_Z to $2M_Z$. At small masses, again, both show large branching ratios for the $b\bar{b}$ decay mode, as well as some for the $c\bar{c}$ and $\tau^+\tau^-$ channels. However, there the similarity ends. The radion Φ has a $\Phi \rightarrow HH$ decay channel, which is obviously forbidden for the Higgs boson. Of greater interest is the loop-mediated decay $\Phi \rightarrow \gamma\gamma$, which is at the level of a few per mil when the radion is light, but is much smaller for a Higgs boson of corresponding mass. (Of course, such light Higgs bosons have not been found at LEP, so this decay mode is not really of much use in distinguishing radions from Higgs bosons.) However, the real *pièce de resistance* is the $\Phi \rightarrow gg$ channel, which has a branching ratio around two orders of magnitude larger than that of the usual $H \rightarrow gg$ process. This branching also dominates when only the trace anomaly contribution is taken and people have presented ways of distinguishing radions and Higgs in this light[13]. Apart from enhancing the branching ratio for a radion decaying to two hadronic jets significantly above the similar decay of the Higgs boson, it reduces, (for a light radion, the branching ratio to a $b\bar{b}$ pair quite significantly.) In fact, we find that for light radions, the *dominant* decay mode is to gluon pairs, while for a light Higgs boson, the dominant decay mode is to $b\bar{b}$. Since the last decay can be pinned down with a fair degree of efficiency by b -tagging methods, we obtain another means of distinguishing between radions and Higgs bosons.

As an example of the efficacy of these ideas, we now consider a 1 TeV linear e^+e^- collider and calculate the production of a radion in association with a Z^0 boson through a process of the form

$$\begin{aligned} e^+e^- &\longrightarrow Z^0 + \Phi \\ &\hookrightarrow \ell^+\ell^- + \Phi \end{aligned}$$

which is then compared with the usual Higgs-strahlung process[14] obtained by replacing Φ by H^0 in the above process and considering the case when the masses and vev's are equal

(or comparable). In the above $\ell = e, \mu, \tau$, and we have folded in the relevant detection efficiencies (i.e. 90% for $\ell = e, \mu$ and 80% for $\ell = \tau$). Of course, there is a fundamental difference in the two cases because the electroweak vev $v_{ew} \simeq 246$ GeV is known, while the radion vev Λ_Φ is an unknown parameter. This feature is also taken care of in our analysis.

The discussion in the preceding paragraph makes it clear that it is interesting to focus on two kinds of final states, viz.

1. $e^+e^- \longrightarrow \ell^+\ell^- + \text{two jets}$, which arises when the scalar particle decays to a pair of light quarks or gluons³, which then undergo fragmentation to form a pair of hadronic jets. Clearly, for a Higgs boson, this final state will receive contributions mainly from the decays $H^0 \rightarrow b\bar{b}$ and $H^0 \rightarrow c\bar{c}$, with a minuscule contribution due to $H^0 \rightarrow gg$. However, the radion decay will have a much larger contribution from the gg mode, and hence the overall branching ratio to jets should be somewhat higher.
2. $e^+e^- \longrightarrow \ell^+\ell^- + b\bar{b}$, which simply means that the final state in the above contains two tagged b -jets. The decay width for $\Phi \rightarrow b\bar{b}$ is roughly the same as that for $H^0 \rightarrow b\bar{b}$ when the masses and couplings are the same. However, the presence of the two-gluon decay mode makes the branching ratio for the $b\bar{b}$ mode fall quite a bit as compared to that for the Higgs boson when the radion is light. Of course, the $b\bar{b}$ cross-section will have to be convoluted with efficiency factors, which we take[15] to be $\eta_b = 0.45$ for each tagged b -quark.

For both kinds of final states, the cross-section will be proportional to, respectively, v_{ew}^{-2} and Λ_Φ^{-2} , and a direct comparison between the Higgs boson and the radion is meaningful only if these match, i.e. $\Lambda_\Phi = v_{ew} \simeq 246$ GeV — a possibility which, though not ruled out, may not, in general, be realised. However, if we consider the *ratio* of the two processes, viz. $\frac{\sigma(e^+e^- \rightarrow \ell^+\ell^- + \text{two jets})}{\sigma(e^+e^- \rightarrow \ell^+\ell^- + b\bar{b})}$ the dependence on the vev cancels out and the differences between the two cases are, therefore, more robust. In fact, the underlying scalar production process being the same, this ratio is more-or-less equal to the ratio of the branching fractions $\frac{B(H/\Phi \rightarrow \text{two jets})}{B(H/\Phi \rightarrow b\bar{b})}$, the only difference being due to efficiency factors.

³We exclude τ^\pm decays because these produce narrow jets which can be identified as τ^\pm with 80-90% efficiency.

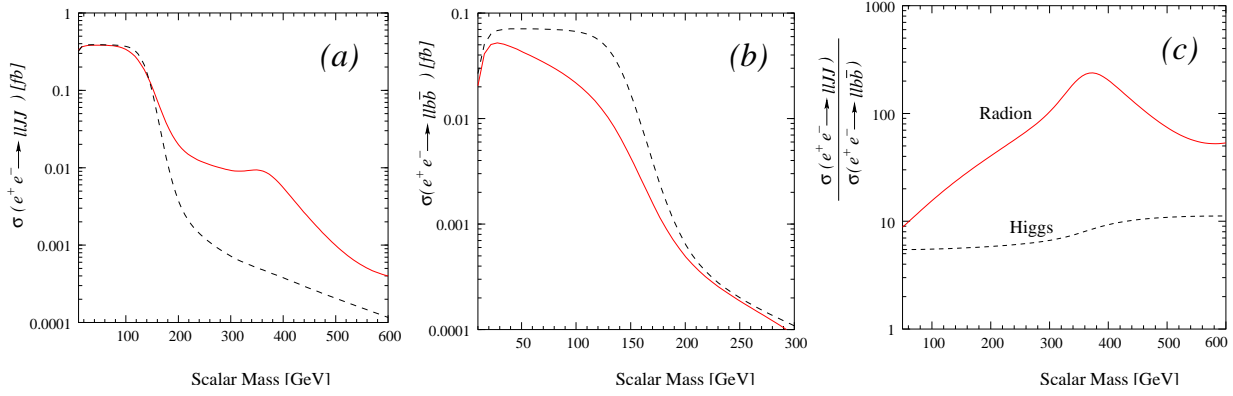


Figure 3. Cross sections (in fb) for radiative scalar production in association with Z^0 bosons, with scalar decay into (a) two jets and (b) two tagged b -jets, as a function of the scalar mass. The solid (red) line denotes the prediction from a radion and the dashed (black) line that from a Higgs boson. We set $\Lambda_\Phi = v_{ew} \simeq 246$ GeV, so that radion and Higgs production cross-sections match. The ratio of the two cross-sections is shown in (c).

In Figure 3 (a) and (b), we illustrate our results for the two processes discussed above, namely,

- (a) $e^+e^- \longrightarrow \ell^+\ell^- + \text{two jets}$, and
- (b) $e^+e^- \longrightarrow \ell^+\ell^- + \text{two } b\text{-jets}$.

The solid (red) line denotes the radion-mediated cross-section, while the dashed (black) line denotes the Higgs-mediated one. In generating the above curves, we have imposed a few kinematic acceptance cuts on the final state particles, viz.,

1. The final-state leptons should have transverse momentum $p_T^{(\ell)} > 20$ GeV.
2. The final-state leptons should have pseudo-rapidity $\eta^{(\ell)} < 2.0$.
3. The final-state jets should be clearly distinguishable by having their thrust axes separated by $\Delta R_{JJ} = \sqrt{\Delta\eta_{JJ}^2 + \Delta\phi_{JJ}^2} > 0.4$, which is the usual criterion adopted at, for example, the LEP and Tevatron colliders.⁴
4. The final-state jets should have transverse momentum $p_T^{(J)} > 10$ GeV.
5. The final-state jets should have pseudo-rapidity $\eta^{(J)} < 2.0$.

The b -tagging efficiency has been taken to be 45%, which is consistent with the LEP value and is probably a conservative estimate than otherwise. It should be noted that the graphs

⁴In a parton-level calculation, this is simply implemented by calculating ΔR for the parent partons, without using a fragmentation algorithm.

show the excess cross-section after removing the non-Higgs part of the Standard Model contributions (such as $e^+e^- \rightarrow ZZ^*$, etc.). These lead to a large SM four-fermion background, which is, however, easily reducible by selecting only events corresponding to peaks in the $\ell^+\ell^-$ and dijet ($b\bar{b}$) invariant masses. We have not exhibited the background analysis in this work because we wish to focus on the *distinction* between the two types of scalar resonances, rather than the mere detection of a scalar resonance (for which several discussions are already available in the literature).

A glance at the cross-sections exhibited in Figure 3 (a) and (b) will make it clear that for scalar masses well below the ZZ -threshold, the cross-sections for $\ell^+\ell^-$ plus two jets final state are almost identical in the two cases, but there is considerable difference if we tag b -jets for scalar masses up to at least 150 GeV. Above the ZZ -threshold there is again significant difference in the total cross-section, which may be attributed to the enhanced decays of the radion to gluon jets. Noting that the plots are semi-logarithmic in nature, the deviations between the two cases are quite large. Interestingly, the two processes complement each other in the sense that each shows a deviation in the mass region where the other process does not. This shows up very clearly in Figure 3 (c), where the ratio of the two cross-sections is plotted and there is a very large deviation between the two cases all through the mass range shown. We thus have a simple and robust method of distinction between production of the two kinds of scalar particle: simply measure the cross sections for $e^+e^- \rightarrow \ell^+\ell^- +$ two jets and for $e^+e^- \rightarrow \ell^+\ell^- +$ two b -jets and compute the ratio. A large ratio (> 10) indicates a radion, while a smaller ratio ($5 - 10$) indicates a Higgs particle. Of course, if the radion vev Λ_Φ is very large, the radion effectively decouples from the Standard Model fields and, though Figure 3 (c) remains unchanged, the radion production cross-sections shown in Figure 3(a, b) dwindle accordingly, so that at some stage they become impossible to measure. This case – though not improbable – is not the point of interest to us in this work.

To summarise, then, this work consists of two parts. In the first part, we have correctly computed the decay width of a radion into two photons or into two gluons using the non-Higgs-like coupling of the radion to off-shell fermions (specifically to off-shell top quarks, in this case). This leads to modest changes in the two-photon branching ratios. However, we predict large changes in the $b\bar{b}$ branching ratio for light radions and to the overall dijet branching ratio for heavy radions, both occurring because of a greatly-enhanced two-gluon decay mode. Using these results, we compute a ‘radion-strahlung’ process at a 1 TeV linear e^+e^- collider and show that the processes $e^+e^- \rightarrow \ell^+\ell^- +$ two jets, with and without

b -tagging, may be used to distinguish signals from the on-shell production of a Higgs boson from those arising from a genuine radion production event. The ratio of the two cases is a robust method to distinguish between the two cases, even if the radion vev Λ_Φ is not well-determined.

Before ending, it needs to be mentioned that we have not taken into account the possibility[16] of *mixing* between the radion and the Higgs boson. This is permissible, and, even if precluded at the tree-level, will be generated by quantum corrections, because the radion and the Higgs boson carry the same set of gauge quantum numbers. In this case, however, it is hardly meaningful to talk of the Higgs boson and the radion separately — there will just be two scalar states of disparate masses, and with couplings scaled suitably by a mixing angle ξ . Our work is, therefore, relevant principally in the limit $\xi \rightarrow 0$. However, it is worth mentioning that even if ξ is finite, the calculation of the decay widths of the new scalar states to a photon pair or a gluon pair, will be along the lines indicated in the present work, and hence, our efforts will not have been entirely in vain.

The authors acknowledge many useful discussions with the late Uma Mahanta, and wish to express a deep sense of loss at his passing. This work is, therefore, dedicated to his memory.

References

- [1] L. Randall and R. Sundrum, *Phys. Rev. Lett.* **83**, 3370 (1999).
- [2] N. Arkani-Hamed, S. Dimopoulos and G.R. Dvali, *Phys. Lett.* **B429**, 263 (1998);
I. Antoniadis, N. Arkani-Hamed, S. Dimopoulos and G.R. Dvali, *Phys. Lett.* **B436**, 257 (1998); N. Arkani-Hamed, S. Dimopoulos and G.R. Dvali, *Phys. Rev.* **D59**, 086004 (1999).
- [3] W.D. Goldberger, M.B. Wise, *Phys. Rev. Lett.* **83**, 4922 (1999).
- [4] W. D. Goldberger, M.B. Wise, *Phys. Rev.* **D60**, 107505 (1999).
- [5] H. Davoudiasl, J.L. Hewett and T.G. Rizzo, *Phys. Rev. Lett.* **84**, 2080 (2000).
- [6] T. Han, J.D. Lykken and R.J. Zhang, *Phys. Rev.* **D59**, 105006 (1999).
- [7] H. Davoudiasl, J.L. Hewett and T.G. Rizzo, *Phys. Rev.* **D63**, 075004 (2001).

- [8] Kingman Cheung, *Phys. Rev.* **D63**, 056007 (2001).
- [9] See, for example, *Current Algebra and Anomalies*, by S. Treiman and R. Jackiw, Princeton University Press (1986).
- [10] U. Mahanta and S. Rakshit, *Phys. Lett.* **B480**, 176 (2000).
- [11] U. Mahanta and A. Datta, *Phys. Lett.* **B483**, 196 (2000).
- [12] V. Barger and R.J.N. Phillips, *Collider Physics*, Addison-Wesley Publishing Company (1987).
- [13] A. Datta and K. Huitu, *Phys. Lett.* **B578**, 376 (2004).
- [14] J.R. Ellis *et al*, *Nucl. Phys.* **B106**, 292 (1976); B.L. Ioffe and V.A. Khoze, *Sov. J. Part. Nucl.* **9**, 50 (1978); B.W. Lee *et al*, *Phys. Rev. Lett.* **38**, 883 (1977).
- [15] See, for example, K. Desch, *Particle Searches at a Linear Collider*, ICHEP2000 (Osaka), 2000.
- [16] G.F. Giudice, R. Rattazzi and J.D. Wells, *Nucl. Phys.* **B595**, 250 (2001); C. Csaki, M. Graesser and G. Kribs, *Phys. Rev.* **D63**, 065002 (2001).